Mon. Not. R. Astron. Soc. **000**, 000–000 (0000) Printed 17 February 2010 (MN LATEX style file v2.2)

Mass-dependent evolution of the relation between supermassive black hole mass and host spheroid mass since z ∼ 1

Shota Kisaka⋆ and Yasufumi Kojima†
Department of Physics, Hiroshima University, Higashi-Hiroshima, Hiroshima 739-8526, Japan

17 February 2010

arXiv:1002.3231v1 [astro-ph.CO] 17 Feb 2010

ABSTRACT

We investigate the evolution of supermassive black hole mass (M_{BH}) and the host spheroid mass (M_{sph}) in order to track the history of the M_{BH}-M_{sph} relationship. The typical mass increase of M_{BH} is calculated by a continuity equation and accretion history, which is estimated from the active galactic nucleus (AGN) luminosity function. The increase in M_{sph} is also calculated by using a continuity equation and a star formation model, which uses observational data for the formation rate and stellar mass function. We find that the black hole to spheroid mass ratio is expected to be substantially unchanged since $z \sim 1.2$ for high mass objects ($M_{BH} > 10^{8.5} M_{\odot}$ and $M_{sph} > 10^{11.3} M_{\odot}$). In the same redshift range, the spheroid mass is found to increase more rapidly than the black hole mass if $M_{sph} > 10^{11} M_{\odot}$. The proposed mass-dependent model is consistent with the current available observational data in the M_{BH}-M_{sph} diagram.

Key words: black hole physics – galaxies:evolution – galaxies:active – quasar:general.

1 INTRODUCTION

Recent observations show that most, if not all, nearby massive spheroids (elliptical galaxies, lenticular and spiral bulges) have supermassive black holes(SMBHs) with masses in the range of $M_{BH} = 10^6$-$10^{10} M_{\odot}$ at their center. In the local universe, the SMBH mass is correlated with characteristic parameters of the host spheroid: the luminosity L_{sph}(Kormendy & Richstone 1995; Marconi & Hunt 2003; Graham 2007), the mass M_{sph} of the spheroid (Magorrian et al. 1998; Häring & Rix 2004), the stellar velocity dispersion σ(Gebhardt et al. 2000; Ferrarese & Merritt 2000; Tremaine et al. 2002) and the various other properties (e.g., Graham et al. (2007); Aller & Richstone (2007); Kisaka, Kojima & Otani (2008)). Understanding the origin of these relations is thought to provide insights into the "co-evolution" of SMBHs and the host spheroids. The role of central black holes in galaxy formation and evolution is not yet established since the SMBH mass is tiny compared with the galaxy as a whole. Areas that are understood at present, as well as those suggested for future observation, were recently reviewed in Cattaneo et al. (2009). Some tentative theories have been proposed to clarify the origin of these correlations (e.g., Silk & Rees (1998)), and they are fairly successful at reproducing the correlations at the present time. However, no theoretical model is widely accepted since there are many unknown parameters in the evolutionary model. For example, in semianalytic models, depending on the model assumptions, the evolution of the scaling relation differs markedly (e.g., Croton (2006); Hopkins et al. (2009)). Therefore, it would be of value to study the evolution using an alternative approach.

Cosmic evolution of the ratio M_{BH}/M_{sph} is observationally studied. McLure et al. (2006) used the 3C RR sample of radio-loud active galactic nuclei (AGNs) for $0 < z < 2$. The number of sources for each redshift bin is not sufficiently large to examine the z-dependence. By fitting data for the relation $M_{BH}/M_{sph} \propto (1+z)^{\gamma}$, the index is estimated as $\gamma = 2$, although data for $z < 1$ are also consistent with no evolution ($\gamma = 0$). Treu et al. (2007) also derived a similar result for SMBH masses in a sample of 20 Seyfert galaxies around $z = 0.36$; however, the evolution was slightly weak, $M_{BH}/M_{sph} \propto (1+z)^{1.5}$. It is not easy at present to judge whether or not cosmological evolution exists, due to several selection biases (Lauer et al. 2007).

⋆ E-mail: kisaka@theo.phys.sci.hiroshima-u.ac.jp
† E-mail: kojima@theo.phys.sci.hiroshima-u.ac.jp

The evolution of the correlations can also be inferred from the demographics of galaxies and AGNs (Merloni, Rudnick & Di Matteo 2004). In some reasonable theories, the nuclear activity of AGNs is proportional to the mass accretion rate into the SMBHs. The luminosity function of AGNs and the redshift evolution measure the buildup of SMBH mass (e.g., Soltan (1982)). The evolution of the galaxies is related to the star formation history. Merloni, Rudnick & Di Matteo (2004) combined the evolution of the SMBH mass density derived from the mass accretion history with that of the stellar mass density derived from the star formation history of the Universe, in order to investigate the evolution of the M_{BH}-M_{sph} relation. They found that the growth of SMBHs appears to predate that of spheroids as $M_{BH}/M_{sph} \propto (1+z)^{0.4-0.8}$, for which the power index of the redshift factor is smaller than that obtained by observations.

Here, we consider the evolutionary model by taking into account the mass-dependent growth in the phenomenological analysis. That is, a simple power-law relation $M_{BH}/M_{sph} \propto (1+z)^{\gamma}$, is not assumed. Only integrated quantities have been used so far in phenomenological studies (e.g., Merloni, Rudnick & Di Matteo (2004)). Our model is an improvement of previous models, in which the mass-dependent effect is now included as an important factor. The mass-dependent property of cosmological evolution is known as "downsizing", in which star formation becomes active in less massive galaxies as the cosmic time increases (e.g., Cowie et al. (1996)). Similarly, an increase in the number of AGNs with redshift compared with the local universe is followed by a decline beyond a peak whose redshift depends on luminosity and hence **on** the SMBH mass, assuming a constant Eddington ratio (e.g., Yencho et al. (2009)). More recently, Labita et al. (2009) have studied the mass dependence of redshift for active black holes by using the Malmquist-bias-unaffected method, and argued that AGN samples at lower redshifts are increasingly dominated by less massive black holes. These observations suggest that the evolution of both SMBH mass and galaxy mass depends on their masses. In this paper, we extend the evolutionary models based on the AGN luminosity function and star formation history by including the mass-dependent effect and derive the evolution of the M_{BH}-M_{sph} relation at certain cosmic ages.

We organize the paper as follows. In Section 2, we briefly review the evolutionary model of SMBHs considered by Marconi et al. (2004); Shankar, Weinberg & Miralda-Escudé (2009), in order to clarify the model parameters. We assume a mean Eddington ratio for the active SMBHs. By adopting a continuity equation and an assumed initial condition, the AGN luminosity function correlates directly with the SMBH mass function at all times. In Section 3, we describe the evolution model of spheroids. Using a method similar to that used for SMBHs, that is, a continuity equation and an assumed initial condition, the stellar mass function and specific star formation rate are used to calculate the mass increase of the spheroids. In Section 4, we combine these two evolutionary models and discuss the evolution of the M_{BH}-M_{sph} relation. Finally in Section 5, we provide a summary. Throughout the paper, we adopt a cosmology with $\Omega_m = 0.3$, $\Omega_\Lambda = 0.7$ and $H_0 = 70$ km s^{-1} Mpc^{-1}.

2 EVOLUTIONARY MODEL OF BLACK HOLES

In the following section, we review the evolutionary equation of the SMBH mass function according to Marconi et al. (2004); Shankar, Weinberg & Miralda-Escudé (2009). The mass of black holes generally increases through mass accretion, which also causes AGN activity. The SMBH mass function is therefore determined from the observed luminosity function of AGNs (e.g., Cavaliere, Morrison & Wood (1971); Small & Blandford (1992); Marconi et al. (2004); Shankar, Weinberg & Miralda-Escudé (2009)). We assume that AGNs are powered by accretion into SMBHs, and that SMBH growth takes place during a phase in which the AGN is shining at a fraction λ of the Eddington luminosity, converting the mass accretion rate with a radiative efficiency ϵ. The number density of SMBHs with mass M_{BH} in co-moving space is denoted by $n(M_{BH},t)$, which satisfies the continuity equation

$$\frac{\partial n(M_{BH},t)}{\partial t} + \frac{\partial}{\partial M_{BH}}[n(M_{BH},t)\langle \dot{M}_{BH}(M_{BH},t)\rangle] = 0, \tag{1}$$

where $\langle \dot{M}_{BH}(M_{BH},t)\rangle$ represents the mean mass-growth rate of M_{BH} at time t. The mass growth is related to AGN activity and hence is expressed by the bolometric luminosity function of the AGNs. Marconi et al. (2004) derived an evolutionary equation of the SMBH number as

$$\frac{\partial n(M_{BH},t)}{\partial t} = -\frac{(1-\epsilon)\lambda^2 c^2}{\epsilon t_{Edd}^2 \ln 10}\left[\frac{\partial \Phi(L_{bol},t)}{\partial L_{bol}}\right], \tag{2}$$

where t_{Edd} is the Eddington time.

The mass growth of SMBHs between redshifts z_1 and z_2 is calculated by the integration

$$\begin{aligned} M(z_2) - M(z_1) &= \int \langle \dot{M}_{BH}(M_{BH},t)\rangle \frac{dt}{dz} dz \\ &= \frac{(1-\epsilon)\lambda}{\epsilon t_{Edd} \ln 10} \int \frac{1}{n(M_{BH},t)}[\Phi(L_{bol},t)]\frac{dt}{dz} dz. \end{aligned} \tag{3}$$

The evolutions of SMBH mass density and typical mass at z are calculated by using eqs. (2) and (3), which are expressed by the AGN luminosity function with two parameters ϵ and λ. We adopt the AGN luminosity function of Shankar, Weinberg & Miralda-Escudé (2009) with a smoothing modification by Raimundo & Fabian (2009). The observed AGN luminosity function is converted to the bolometric luminosity by using the luminosity-dependent correction of Marconi et al. (2004). The initial condition for the integration of eq. (3) is chosen as the condition at $z = 6$, which is the same as Shankar, Weinberg & Miralda-Escudé (2009). They noted that the integration does not significantly depend on the initial value after $z \sim 3.5$ unless the SMBH duty cycle is extremely small.

In order to constrain the free parameters ϵ and λ, we compare the local SMBH mass function derived from the evolution model with an observational value. Shankar, Weinberg & Miralda-Escudé (2009) carried out a detailed comparison by using the SMBH mass function derived by various methods. We also obtained the same results as Shankar, Weinberg & Miralda-Escudé (2009), even when including the technical smoothing modification. The best-fitting values are $\epsilon = 0.065$ and $\lambda = 0.42$. Uncertainty in the radiative efficiency ϵ is not a highly important parameter affecting the mass growth of SMBHs since it affects only the overall normalization. The parameter is fixed as $\epsilon = 0.065$ from now on. The Eddington ratio λ is a critical parameter describing SMBH evolution. Shankar, Weinberg & Miralda-Escudé (2009) estimated a reasonable range of their model parameter, which is converted as $\lambda = 0.28$-0.56. The range implies not uncertainty in any statistical sense, but rather a preferable range.

In Figure 1, we plot the averaged growth history of SMBHs with different masses for $0 < z < 1.2$. The mass range of black holes for which current observational data are available is limited to $10^7 < M_{BH}/M_\odot < 10^{9.5}$. It is clear that the growth depends on black hole mass. A black hole with $M_{BH} \sim 10^7 M_\odot$ rapidly increases its mass from $z = 1.2$ to $z = 0$, while one with $M_{BH} \sim 10^9 M_\odot$ stops its growth at $z = 1.2$. We also demonstrate the upper and lower limits of the Eddington ratio for two representative evolutionary tracks as shaded areas. One is the track of $M_{BH} = 10^{8.5} M_\odot$ at $z = 0$, and the other is $M_{BH} = 10^{7.5} M_\odot$. We find that the uncertainty is important around the bend of the curve, where the growth is rapid. The uncertainty does not seriously affect the evolution for $M_{BH} > 10^8 M_\odot$. The uncertainty in the track of less massive black holes can be clearly seen, for example, ~ 0.4dex in $\log M_{BH}$ for $M_{BH} = 10^{7.5} M_\odot$ at $z = 0.9$.

3 EVOLUTIONARY MODEL OF SPHEROIDS

In this section, we introduce a simple model of spheroid mass evolution. It is well known that galaxies form two sequences in color-magnitude space: star-forming, late-type galaxies occupy the blue cloud, whereas quiescent, bulge-dominated early-type galaxies reside on the red sequence (e.g., Bell et al. (2004)). We focus on early type galaxies and derive the spheroid mass evolution assuming a fixed bulge-to-total ratio (B/T).

We use the method reported by Bell et al. (2007) to determine the evolution of the stellar mass function. The number densities of both the early- and late-type galaxies, respectively, satisfy the continuity equation with a source function S for each type as

$$\frac{\partial n_{early}(M,t)}{\partial t} + \frac{\partial}{\partial M}[n_{early}(M,t)\dot{M}_{early}(M,t)] = S_{early}(M,t), \tag{4}$$

$$\frac{\partial n_{late}(M,t)}{\partial t} + \frac{\partial}{\partial M}[n_{late}(M,t)\dot{M}_{late}(M,t)] = S_{late}(M,t). \tag{5}$$

For all galaxies, we have

$$\frac{\partial n_{all}(M,t)}{\partial t} + \frac{\partial}{\partial M}[n_{all}(M,t)\dot{M}_{all}(M,t)] = S_{all}(M,t), \tag{6}$$

where

$$n_{all}(M,t) = n_{early}(M,t) + n_{late}(M,t), \tag{7}$$

$$n_{all}(M,t)\dot{M}_{all}(M,t) = n_{early}(M,t)\dot{M}_{early}(M,t) + n_{late}(M,t)\dot{M}_{late}(M,t), \tag{8}$$

$$S_{all}(M,t) = S_{early}(M,t) + S_{late}(M,t). \tag{9}$$

Bell et al. (2007) calculated the evolution of the mass function for all galaxies with an assumption $S_{all} = 0$, and found that the results were consistent with the observational COMBO-17 data at $0.2 < z < 1.0$ (Borch et al. 2006). They also found $\partial n_{late}/\partial t = 0$ by comparing the observed mass function of all galaxies with that of late-type galaxies between $z = 0$ and $z \sim 0.9$. We adopt both conditions in our analysis. The continuity can be written as

$$\begin{aligned} \frac{\partial n_{early}(M,t)}{\partial t} &= -\frac{\partial}{\partial M}[n_{all}(M,t)\dot{M}_{all}(M,t)] \\ &= -\frac{\partial}{\partial M}[n_{early}\langle\dot{M}_{early}(M,t)\rangle], \end{aligned} \tag{10}$$

where

$$\langle \dot{M}_{early}(M,t) \rangle = \frac{n_{all}(M,t)}{n_{early}(M,t)} \dot{M}_{all}(M,t). \tag{11}$$

The typical mass of the early-type galaxies is obtained by integrating the equation

$$M_{early}(z_2) - M_{early}(z_1) = \int \langle \dot{M}_{early}(M,t) \rangle \frac{dt}{dz} dz. \tag{12}$$

The spheroid mass evolution is determined from the stellar mass function of early-type galaxies adopting B/T=0.7, which does not depend on the redshift or galaxy mass (see Tamura, Ohta & Ueda (2006)).

The mass increase $\dot{M}_{all}$ is determined by the star formation rate. We adopt the staged τ model introduced by Noeske et al. (2007) and use the same values and uncertainty ranges. The main model parameters are c_α and c_β, which control the gas exhaustion timescale and the formation redshift, respectively. The model by Noeske et al. (2007) is consistent with observations over a wide range of masses and may be used as a well-fitting formulation of specific star formation rate (SSFR). Figure 2 shows the SSFR Ψ/M at z =0.3, 0.5, 0.7 and 0.9. Here we include much more observational data, and obtain the same results as Noeske et al. (2007). For the stellar mass function data, we use the data of Ilbert et al. (2010) from the COSMOS survey covering 2-deg^2, in which morphological and spectral classifications were carried out. The combined classifications allow us to isolate the "blue elliptical" galaxies that are not included in the red sequence. We use the early-type (elliptical in Ilbert et al. (2010)) galaxy mass function at $z \leq 1.2$ as the spheroid mass function.

The mass evolution is determined by easily integrating eq. (12) since eq. (11) is expressed as a smooth curve. The results are shown in Figure 3. It is found that there is no significant growth in the mass range of $M \geq 10^{11} M_\odot$. As discussed regarding the evolution of SMBHs, uncertainty in the model parameters is important in the phase of rapid growth. The parameters of spheroid evolution are the B/T ratio, and the SSFR parameters (c_α and c_β). We use B/T=0.7, but examine the variation for 0.4< B/T <1, which Im et al. (2002) considered as a reasonable range. The range of variation is shown for two evolutionary tracks in Figure 3. The uncertainty in $\log M_{sph}$ for $M_{sph} = 10^{10.3} M_\odot$ at $z = 0.9$ is ~ 0.6dex. This uncertainty can be neglected for $M_{sph} > 10^{11} M_\odot$. We also examine the variation due to the SSFR parameters in Figure 4. It is found that the variation in the SSFR parameters affects the evolution more strongly than that in the B/T ratio. However, neither affects the spheroid evolution for $M_{sph} > 10^{11.5} M_\odot$.

4 RESULTS

4.1 Evolution of the M_{BH}-M_{sph} relation

The combination of models for SMBH mass and spheroid mass allows us to investigate the mass-dependent evolution of the M_{BH}-M_{sph} relation. In the local universe, the M_{BH}-M_{sph} relation found by Häring & Rix (2004) satisfies

$$\log(M_{BH}/M_\odot) = 8.20 + 1.12 \log(M_{sph}/10^{11} M_\odot). \tag{13}$$

Using this, we consider the relation at $0 < z < 1.2$. Figure 5 shows our results for a reference model with $\lambda = 0.42$, B/T=0.7, $c_\alpha = 10^{20.7}$ and $c_\beta = 10^{-2.7}$. In order to account for the intrinsic scatter at $z = 0$, we add an offset of ± 0.3dex (Häring & Rix 2004) in eq. (13), so that two curves corresponding to upper and lower limits are also plotted at each value of z. We found that the M_{BH}-M_{sph} relation does not change since $z \sim 1.1$ in the region for $M_{BH} \gtrsim 10^{8.5} M_\odot$ and $M_{sph} \gtrsim 10^{11.3} M_\odot$. The reason is clear in Figures 1 and 3, where no evolution was seen in either mass on the massive side. On the other hand, there is a significant deviation from the linear relation when $M_{BH} < 10^8 M_\odot$. This denotes that a massive BH with $M_{BH} = 10^8 M_\odot$ is already located at a relatively small spheroid mass of $M_{sph} = 10^{10.5} M_\odot$ at $z \sim 1$. The spheroid mass subsequently increases to $M_{sph} = 10^{10.8} M_\odot$, while M_{BH} is fixed at $10^8 M_\odot$. In order to evaluate the increase of the SMBH mass for a fixed spheroid mass M_{sph}, we consider the difference $\Delta \log(M_{BH}) = \log(M_{BH}(z)/M_{BH}(0))$. When the evolution is plotted as $\log(1+z)^\gamma$, we obtain $\gamma = 2.11$ at $M_{sph} = 10^{10} M_\odot$, $\gamma = 1.05$ at $M_{sph} = 10^{10.5} M_\odot$ and $\gamma = 0.43$ at $M_{sph} = 10^{11} M_\odot$. In the higher-mass regime of $M_{sph} > 10^{11} M_\odot$, no significant evolution is found. Thus, the evolution of the M_{BH}-M_{sph} relation at $z \lesssim 1.1$ clearly depends on the mass range. The growth is more rapid for a smaller spheroid mass. If we integrate the relation with the mass function over the whole mass range, then the averaged power index becomes $\gamma \sim 0.8$. We show the relation with $\gamma = 0.8$ for comparison in subsection 4.2 (Figure 8). This parameterization for evaluating cosmological evolution has been used by Merloni, Rudnick & Di Matteo (2004), and our result is consistent with their value within an error of 1σ. The index of the average is almost the same as that of the previous phenomenological model (e.g., Merloni, Rudnick & Di Matteo (2004)), but mass-dependent evolution, especially at lower mass, is a remarkable new property in our model.

In order to compare the growth of SMBHs and spheroids, we present two extreme cases in Figure 6. One is calculated without evolution of SMBHs, and the other is calculated without evolution of spheroids. Both two curves deviate from our reference model as well as from the M_{BH}-M_{sph} relation at $z = 0$, as z increases. The deviation is remarkable at lower mass. However, our reference model is close to the curve for no evolution of SMBHs. This means that the mass increase of the spheroids around $M_{sph} = 10^{10.5} M_\odot$ is more rapid.

We examine the model parameters discussed in Section 2 and 3 to demonstrate deviation from the reference model. The three parameters are independent and the results change monotonically as each parameter is changed. Thus, we have calculated two extreme cases: upper and lower limits of the M_{BH}-M_{sph} relation. These results are shown in Figure 7. For the model with $c_\alpha = 10^{20.7}$ and $c_\beta = 10^{-3.0}$, which corresponds to the curve for the upper limit in Figure 7, the distribution of M_{BH} in the range of $M_{sph} \lesssim 10^{11} M_\odot$ is a nearly horizontal line at $z \sim 1.1$. On the other hand, for $c_\alpha = 10^{20.4}$ and $c_\beta = 10^{-1.7}$, corresponding to the curve for the lower limit in Figure 7, the distribution in the same range is even lower than that of the local relation. For lower masses, the deviation from the linear line is general, and the typical SMBH mass depends on the model. For example, our model shows that M_{BH} ranges from $10^7 M_\odot$ to $10^{8.5} M_\odot$ for $M_{sph} = 10^{10.5} M_\odot$ at $z = 1$. The possible range of masses is wide, but our reference model, which can be regarded as an average of two extreme cases, suggests slightly larger SMBH mass than that of the local universe relation. It is also found that the relation is not affected in the mass range of $M_{sph} \gtrsim 10^{11.5} M_\odot$.

4.2 Comparison with observations

In this subsection, we compare our model with observational results available in the literature. McLure et al. (2006) investigated the evolution of the SMBH-to-host galaxy mass ratio in the redshift range of $0 < z < 2$. They estimated the masses M_{BH} for the 3C RR quasars and spheroid masses M_{sph} for the 3C RR radio galaxies. Two samples are not the same, but the averaged mass was determined. Recently, Decarli et al. (2009b) studied the redshift dependence of the relation up to $z = 3$ using a sample of 96 quasars for which the host galaxy luminosity is known. They listed M_{BH} and M_{sph} for each source. Both results are used for comparison after we derive M_{BH} from the observational data by the same method. Black hole masses are usually estimated by the virial method (e.g., McLure & Jarvis (2002); Kollmeier et al. (2006)). The masses are derived from the broad emission-line width v as a velocity indicator, and the monochromatic continuum luminosity L is used as an indicator of the region size:

$$\log M_{BH} = A + 2 \log v + B \log L, \tag{14}$$

where A and B are constants. The line width v is typically taken from the broad line of Mg_{II} or Hβ, and the luminosity L is taken at 3000Åor 5100Å. The constants A and B have not been determined with high accuracy, since the best fit values slightly depend on observational choices of v and L. The black hole masses are derived by a different choice of A and B in the works of McLure et al. (2006) and Decarli et al. (2009b). It is preferable to use a single formula for the estimation. One possible approach is to use the values, A and B, derived by McGill et al. (2008), who cross-calibrated a number of different formulae in a redshift range where more than one broad emission line could be observed simultaneously in optical spectra. We adopt their calibrated values for A and B, in order to re-derive black hole masses. We calculate M_{BH} of the objects in the samples by McLure et al. (2006) and Decarli et al. (2009b), for which the line width of Mg_{II} or Hβ is measured. The corresponding line width of nine objects is not listed; consequently, these are excluded from our analysis. In Figure 8, we plot (M_{BH}, M_{sph}) not for each source but for the average, since we focus only on statistical properties. Our values M_{BH} and those listed in McLure et al. (2006) and Decarli et al. (2009b) are not notably different by averaging. Bennert et al. (2010) investigated the evolution of the M_{BH}-L_{sph} relation. [1] As discussed previously, M_{BH} is derived from spectral data using the mass estimator by McGill et al. (2008). The spheroid mass M_{sph} is derived from L_{sph} and the mass-to-light ratio by a certain stellar population model(Bruzual & Charlot (2003)). Thus, converted data are also plotted in Figure 8. We group data into two ranges, $M_{sph} < 10^{11} M_\odot$ and $M_{sph} \geq 10^{11} M_\odot$, and respectively average M_{BH} and M_{sph}, since the sample number is small. Although detailed comparison is difficult due to the small sample and the ambiguity in the conversion relation, the results are consistent with mass-dependent evolution. The samples are deawn from the high mass end of the spheroid mass function ($M_{sph} > 10^{11.5} M_\odot$), where we expect little or no evolution in the M_{BH}-M_{sph} relation since $z \sim 1$. Comparing our evolutionary model with observations in each redshift bin we find consistency with observations, although we cannot exclude a mass-independent scenario because of the lack of observational data in the low spheroid mass range.

We next consider additional observation data, although the comparison becomes indirect. Salviander et al. (2007) investigated the evolution of the M_{BH}-σ relation. An evolutionary model of σ is necessary, but here we assume that the conversion relation from σ to M_{sph} is the same as that of $z = 0$. In other words, the relation between σ and M_{sph} at $z = 0$ is derived by eliminating M_{BH} in eq. (13) and the M_{BH}-σ relation at $z = 0$ by Tremaine et al. (2002), and the relation is assumed to hold for all z. Averaged data points from Salviander et al. (2007) are also plotted in Figure 8. These data correspond to small masses of $M_{sph} < 10^{11} M_\odot$ and show relatively strong evolution, supporting the hypothesis of a mass-dependent evolution scenario.

[1] Similar samples were previously given by Treu et al. (2007), but most of these were covered by the sample of Bennert et al. (2010).

5 SUMMARY AND CONCLUSIONS

We have modeled the mass-dependent evolution of black holes and spheroids since $z \sim 1.2$. The black hole mass evolution was investigated by using a continuity equation and the observed AGN luminosity function. The spheroid mass evolution was also derived from a continuity equation and the observed SSFR. Both evolutions, which were consistent with "downsizing", significantly depend on the masses of the SMBHs and spheroids, and the M_{BH}-M_{sph} relation is mass-dependent. We assumed that all galaxies at $z = 0$ satisfy the linear relation of the $\log(M_{BH})$-$\log(M_{sph})$ diagram with some uncertainty, and examined the history to $z \sim 1.2$. It was found that the relation is unchanged for $0 < z < 1.2$ in the range of $M_{BH} > 10^8 M_\odot$ and $M_{sph} > 10^{11} M_\odot$. In the low-mass regime, however, there is clear deviation from the linear relation. The mass increase of the spheroids is likely larger than that of black holes, although there is uncertainty in the model parameters. Our model suggests that SMBHs were already located in spheroids with relatively small mass, compared with the local relation.

We also compared our results with currently available observations concerning the relations between M_{BH} and host spheroid parameters at certain cosmic ages. Our mass-dependent evolutionary model is consistent with these observations, although the observational sample is not sufficiently complete to make a statistically significant comparison. Larger observational samples are needed to study the history of SMBHs and their hosts statistically, expecially in the low-mass regime where the differences between the mass-dependent and the mass-independent evolution models are higher. If a break from the linear $\log(M_{BH})$-$\log(M_{sph})$ is found, our mass-dependent scenario would be supported and it would be possible to put stronger constraints on model parameters. It would also be of great interest to extend the present results to higher redshift, where the model uncertainties are considerably smaller. This would enable us to reveal possible inconsistencies between model and observations. However, the extension of the present study to higher redshift is not straightforward, as the adopted stellar mass function for early-type galaxies is only significant at $z < 1.2$ (Ilbert et al. 2010).

REFERENCES

Aller, M. C., & Richstone, D. O. 2007, ApJ, 665, 120
Bell, E. F., Zheng, X. Z., Papovich, C., Borch, A., Wolf, C., & Meisenheimer, K. 2007, ApJ, 663, 834
Bell, E. F., et al. 2004, ApJ, 608, 752
Bennert, V. N., et al. 2010, ApJ, 708, 1507
Borch, A., Meisenheimer, K., Bell, E. F., Rix, H.-W., Wolf, C., Dye, S., Kleinheinrich, M., & Kovacs, Z. 2006, A&A, 453, 869
Bruzual, G., & Charlot, S. 2003, MNRAS, 344, 1000
Buat, V., et al. 2008, A&A, 483, 107
Cattaneo, A., et al. 2009, Nature, 460, 213
Cavaliere A., Morrison, P., & Wood, K. 1971, ApJ, 170, 223
Chen, Y.-M., Wild, V., Kauffmann, G., Blaizot, J., Davis, M., Noeske, K., Wang, J.-M., & Willmer, C. 2009, MNRAS, 393, 406
Cowie, L. L., Songaila, A., Hu, E. M., & Cohen, J. G. 1996, AJ, 112, 839
Croton, D. J. 2006, MNRAS, 369, 1808
Damen, M., Labbé, I., Franx, M., van Dokkun, P. G., Taylor, E. N., & Gawiser, E. J. 2009, ApJ, 690, 937
Decarli, R., Falomo, R., Treves, A., Labita, M., Kotilainen, J.K., & Scarpa, R. 2009, MNRAS, accepted (arXiv:0911.2988)
Ferrarese, L., & Merritt, D. 2000, ApJ, 539, L9
Gebhardt, K., et al. 2000, ApJ, 539, L13
Graham, A. W. 2007, MNRAS, 379, 711
Graham, A. W., Driver, S. P., Allen, P. D., & Liske, J. 2007, MNRAS, 378, 198
Häring , N., & Rix, H.-W. 2004, ApJ, 604, L89
Hopkins, P. F., Hernquist, L., Cox, T. J., Keres, D. & Wuyts, S. 2009, ApJ, 691, 1424
Iglesias-Páramo, J., et al. 2007, ApJ, 670, 279
Ilbert, O., et al. 2010, ApJ, 709, 644
Im, M., et al. 2002, ApJ, 571, 136
Kisaka, S., Kojima, Y., & Otani, Y. 2008, MNRAS, 390, 814
Kollmeier, J. A., et al. 2006, ApJ, 648, 128
Kormendy, J., & Richstone, D. 1995, ARA&A, 33, 581
Labita, M., Decarli, R., Treves, A., & Falomo, R. 2009, MNRAS, 396, 1537
Lauer, T. R., Tremaine, S., Richstone, D., & Faber, S. M. 2007, 670, 249
Magorrian, J., et al. 1998, AJ, 115, 2285
Marconi, A., & Hunt, L. K. 2003, ApJ, 589, L21
Marconi, A., Risaliti, G., Gilli, R., Hunt, L. K., Maiolino, R., & Salvati, M. 2004, MNRAS, 351, 169

Martin, D. C., et al. 2007, ApJS, 173, 415
McGill, K. L., Woo, J.-H., Treu, T., & Malkan, M. A. 2008, ApJ, 673, 703
McLure, R. J., & Jarvis, M. J. 2002, MNRAS, 337, 109
McLure, R. J., Jarvis, M. J., Targett, T. A., Dunlop, J. S., & Best, P. N., 2006, MNRAS, 368, 1395
Merloni, A., Rudnick, G., & Di Matteo, T. 2004, MNRAS, 354, L37
Noeske, K. G., et al. 2007, ApJ, 660, L47
Pannella, M., Hopp, U., Saglia, R.P., Bender, R., Drory, N., Salvato, M., Gabasch, A., & Feulner, G. 2006, ApJ, 639, L1
Pérez-González, P. G., et al. 2008, ApJ, 675, 234
Raimundo, S. I., & Fabian, A. C. 2009, MNRAS, 396, 1217
Salviander, S., Shields, G. A., Gebhardt, K., & Bonning, E. W. 2007, ApJ, 662, 131
Shankar, F., Weinberg, D. H., & Miralda-Escudé, J. 2009, ApJ, 690, 20
Silk, J., & Rees, M., J. 1998, A&A, 331, L1
Small, T. A., & Blandford, R. D. 1992, MNRAS, 259, 725
Soltan, A. 1982, MNRAS, 200, 115
Tamura, N., Ohta, K., & Ueda, Y. 2006, MNRAS, 365, 134
Tremaine, S., et al. 2002, ApJ, 574, 740
Treu, T., Woo, J.-H., Malkan, M. A., & Blandford, R. D. 2007, ApJ, 667, 117
Ueda, Y., Akiyama, M, Ohta, K., & Miyaji, T. 2003, ApJ, 598, 886
Yencho, B., Barger, A. J., Trouille, L. & Winter, L. M. 2009, ApJ, 698, 380
Zheng, X. Z., Bell, E. F., Papovich, C., Wolf, C., Meisenheimer, K., Rix, H.-W., Rieke, G. H., & Somerville, R. 2007, ApJ, 661, L41

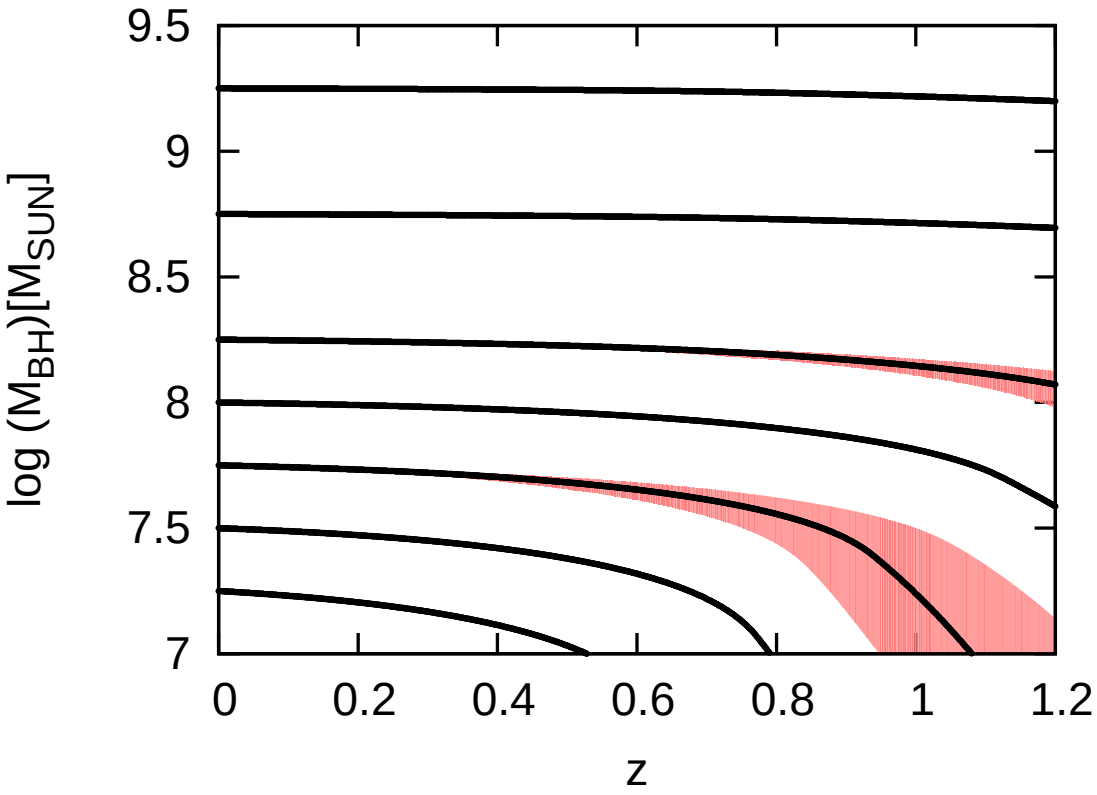

Figure 1. Averaged growth history of SMBHs computed using AGN luminosity function and $\epsilon = 0.065$. Eddington ratio is λ =0.42. Red shaded areas show the difference in $\log M_{BH}$ between $\lambda = 0.56$ and $\lambda = 0.28$ for representative tracks at z =0.3, 0.5, 0.7, 0.9 and 1.1.

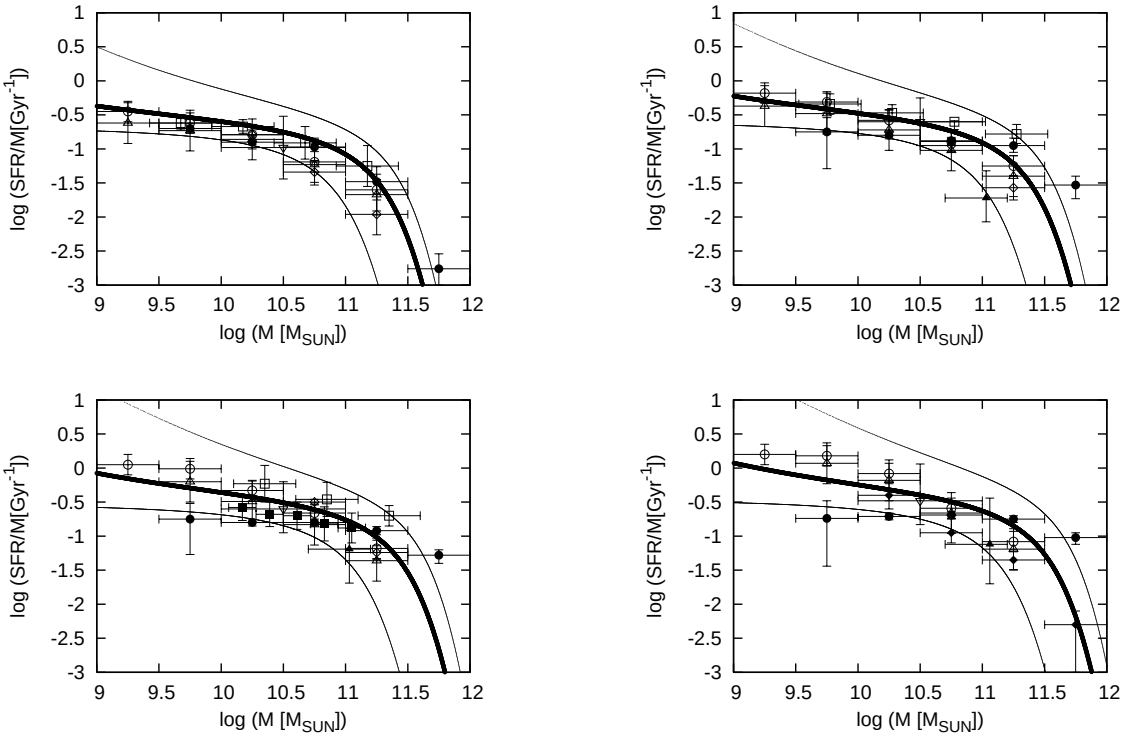

Figure 2. Specific star formation rate as a function of stellar mass from $z = 0.3$ (upper left), $z = 0.5$ (upper right), $z = 0.7$ (lower left) and $z = 0.9$ (lower right). Thick lines show staged τ models and thin-lines show effect of varying c_α and c_β (or, z_f and τ). Fitting parameters are given in Noeske et al. (2007). Data points correspond to measurements from Zheng et al. (2007)(open circles), Martin et al. (2007)(closed circles), Iglesias-Páramo et al. (2007)(open squares), Buat et al. (2008)(closed squares), Bell et al. (2007)(open upward triangles), Pannella et al. (2006)(closed upward triangles), Damen et al. (2009) (open diamonds), Chen et al. (2009)(closed diamonds) and Pérez-González et al. (2008)(open downward triangles).

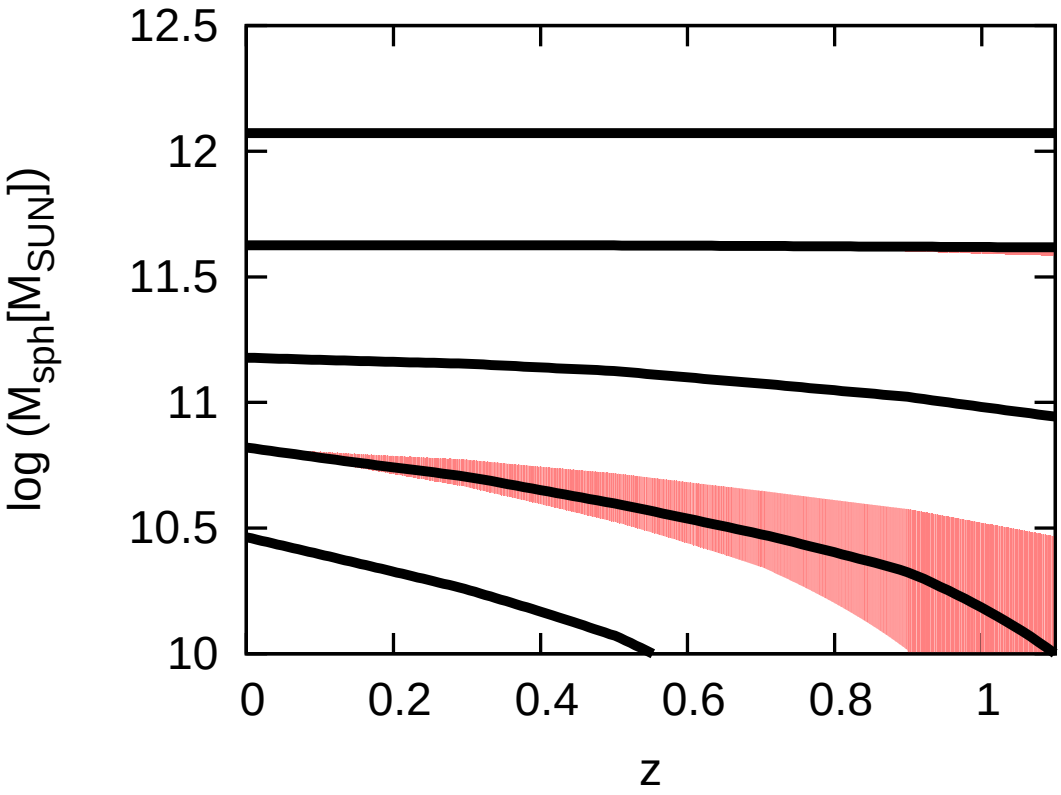

Figure 3. Averaged growth history of spheroids computed using B/T=0.7 and SSFR with $c_\alpha = 10^{20.7}$ and $c_\beta = 10^{-2.7}$. Red shaded areas show the difference in $\log M_{sph}$ between B/T=0.4 and B/T=1.0 for representative tracks at z =0.3, 0.5, 0.7, 0.9 and 1.1.

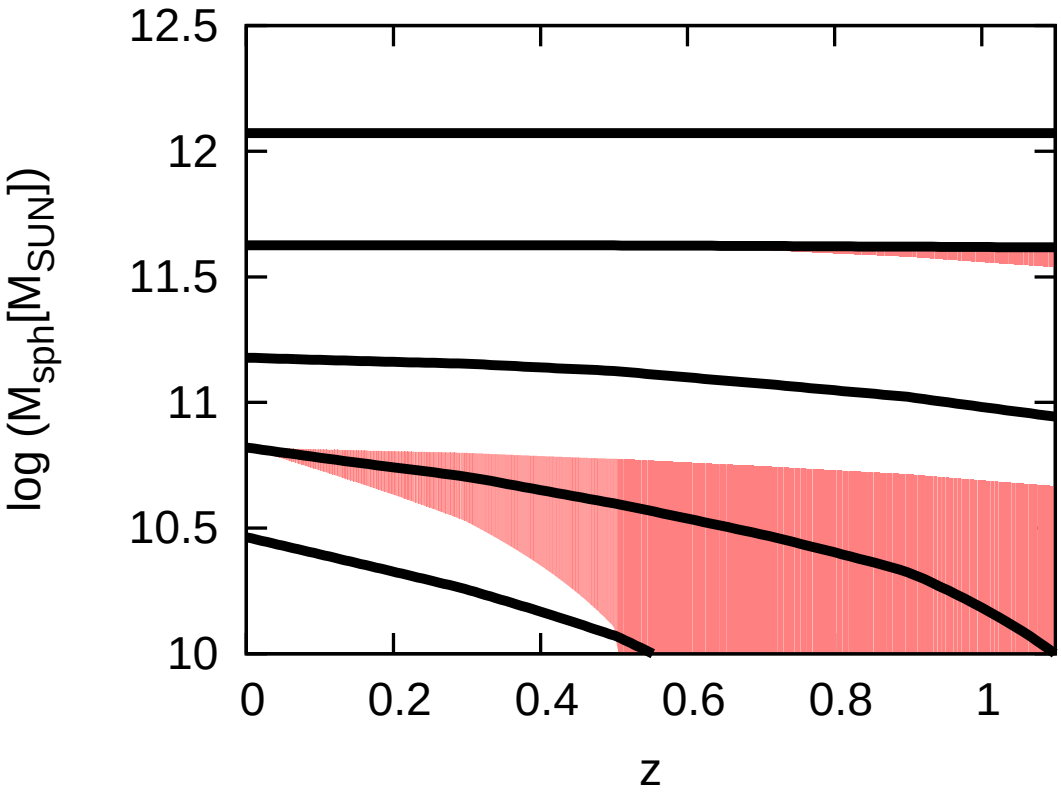

Figure 4. Averaged growth history of spheroids computed using B/T=0.7 and SSFR parameters (c_α, c_β) with ($10^{20.7}$, $10^{-2.7}$). Red shaded areas show the difference in $\log M_{sph}$ between (c_α, c_β)=($10^{20.4}$, $10^{-1.7}$) and ($10^{20.7}$, $10^{-3.0}$) for representative tracks at z =0.3, 0.5, 0.7, 0.9 and 1.1.

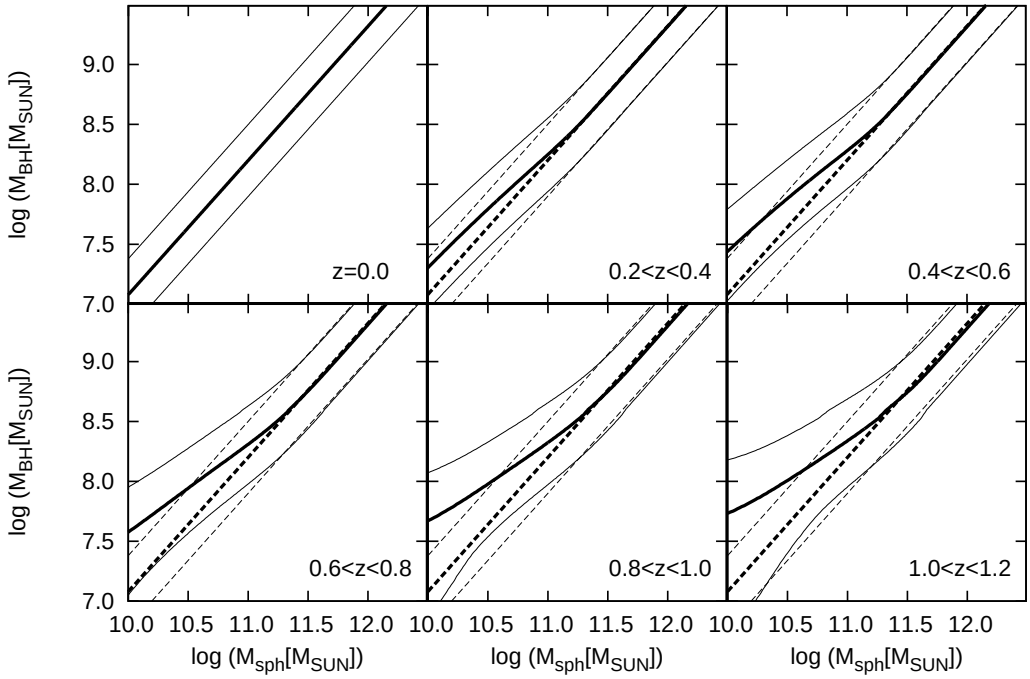

Figure 5. Evolution of M_{BH}-M_{sph} relation from $z \sim 1.2$ to $z = 0$. Model parameters are $\lambda = 0.42$, B/T=0.7, $c_\alpha = 10^{20.7}$ and $c_\beta = 10^{-2.7}$. An offset ± 0.3dex is added due to scatter in the local M_{BH}-M_{sph} relation. Relation, and upper and lower limits at $z = 0$ are plotted by thick dotted lines and thin dotted lines, respectively.

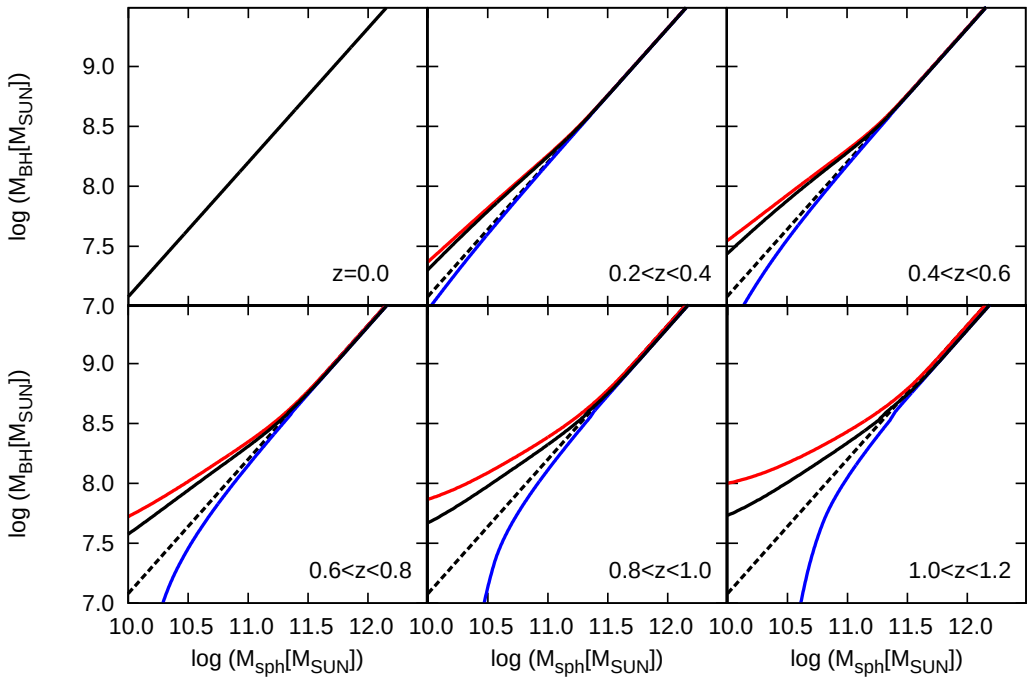

Figure 6. Comparison of evolutionary models of M_{BH}-M_{sph} relation. Black solid line is our reference model; black dotted line is relation at $z = 0$. Model with fixed SMBH mass is denoted by top (red) line; model with fixed spheroid mass is denoted by bottom (blue) line.

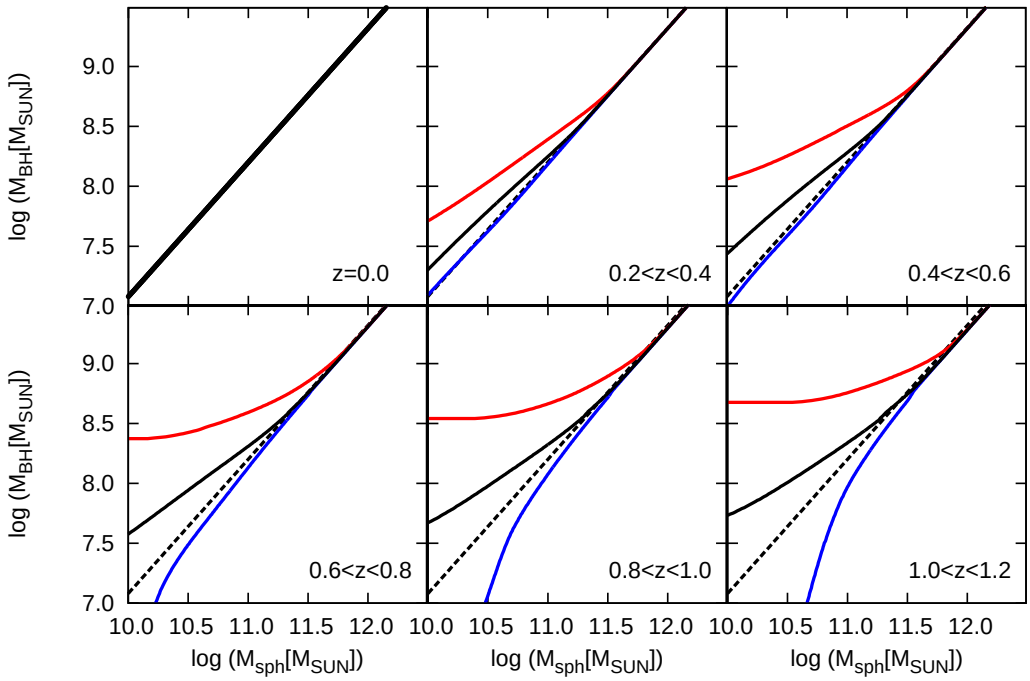

Figure 7. Evolution of M_{BH}-M_{sph} relation from $z \sim 1.2$ to $z = 0$ varying model parameters. Black solid line is our reference model; black dotted line is M_{BH}-M_{sph} relation at $z = 0$. Top (red line) is upper limit, for which $\lambda = 0.28$, B/T=0.4, $c_\alpha = 10^{20.4}$ and $c_\beta = 10^{-1.7}$; Bottom (blue line) is lower limit, for which $\lambda = 0.56$, B/T=1.0, $c_\alpha = 10^{20.7}$ and $c_\beta = 10^{-3.0}$.

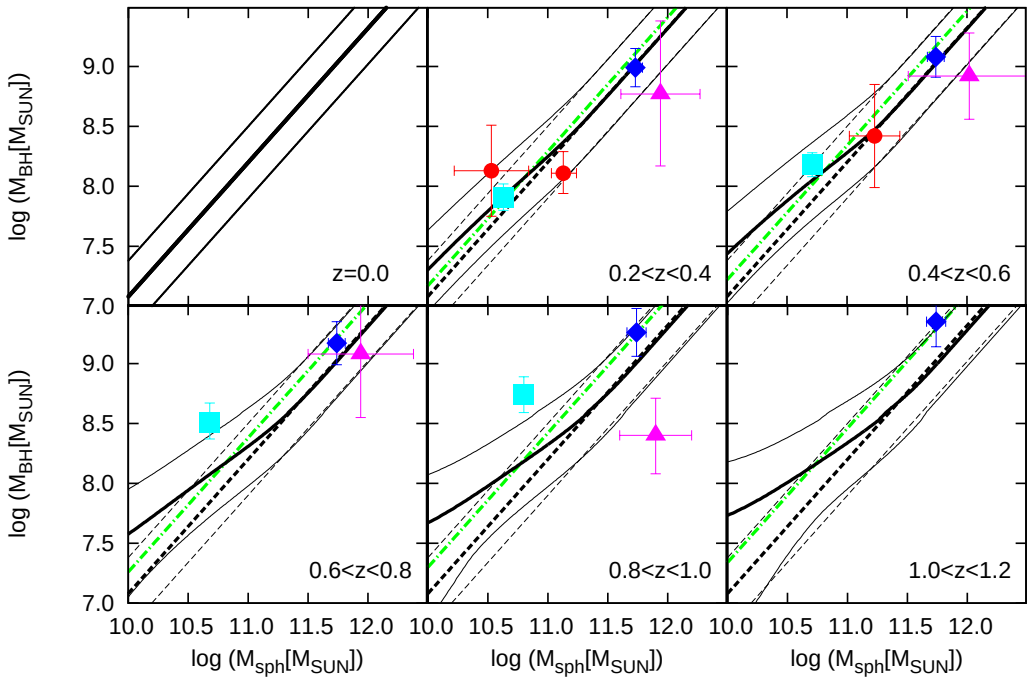

Figure 8. Comparison of M_{BH}-M_{sph} relation from $z \sim 1.2$ to $z = 0$ with observations. Solid lines are reference models and dotted lines are local relations. The relation shifted by $(1+z)^{0.8}$ is shown by dash-dotted (green) lines. Red circles: Bennert et al. (2010); light blue squares: Salviander et al. (2007); purple triangles: Decarli et al. (2009b); blue diamonds: McLure et al. (2006). Error bars are standard deviation of the logarithmic mean.